Research Article

Palaeohydrogeology and Transport Parameters Derived from ^{4}He and Cl Profiles in Aquitard Pore Waters in a Large Multilayer Aquifer System, Central Australia

Stacey C. Priestley,[1] Tavis Kleinig,[2] Andrew J. Love,[1] Vincent E. A. Post,[1] Paul Shand,[1,3] Martin Stute,[4,5] Ilka Wallis,[1] and Daniel L. Wohling[2]

[1]*School of the Environment, Flinders University, Earth Sciences Building, Bedford Park, SA 5042, Australia*
[2]*Department of Environment, Water and Natural Resources, Government of South Australia, Adelaide, SA 5000, Australia*
[3]*CSIRO Land and Water, Urrbrae, SA 5064, Australia*
[4]*Lamont-Doherty Earth Observatory, Columbia University, Palisades, NY 10964, USA*
[5]*Barnard College, New York City, NY 10027, USA*

Correspondence should be addressed to Stacey C. Priestley; stacey.priestley@flinders.edu.au

Received 1 June 2017; Accepted 2 October 2017; Published 20 November 2017

Academic Editor: Douglas K. Solomon

A study of chloride and ^{4}He profiles through an aquitard that separates the Great Artesian Basin from the underlying Arckaringa Basin in central Australia is presented. The aquitard separates two aquifers with long water residence times, due to low recharge rates in the arid climate. One-dimensional solute transport models were used to determine the advective flux of groundwater across the aquitard as well as establish any major changes in past hydrological conditions recorded by variations of the pore water composition. This *in situ* study showed that both diffusion and slow downward advection (v_z = 0.7 mm/yr) control solute transport. Numerical simulations show that an increase in chloride concentration in the upper part of the profile is due to a reduction in recharge in the upper aquifer for at least 3000 years. Groundwater extraction since 2008 has likely increased chloride and ^{4}He concentrations in the lower aquifer by pulling up water from deeper layers; however, there has been insufficient time for upward solute transport into the pore water profile by diffusion against downward advection. The transport model of ^{4}He and chloride provides insight into how the two aquifers interact through the aquitard and how climate change is being recorded in the aquitard profile.

1. Introduction

Aquitards, that is, low permeability geological formations, play an important role in the physical and chemical evolution of groundwater. They control the response of aquifers to forcing, such as pumping, and impede the movement of water between aquifers [1, 2]. They also exert a strong influence on solute migration and can sequester solutes, with important implications for contaminant migration as well as for isotope tracer studies [3–5]. Understanding the hydrological role of aquitards is vital in areas impacted by large-scale groundwater abstraction, for example, mining activities, and for safety assessment studies of waste repositories. Despite this, aquitards remain less well studied in comparison to aquifers because of the inherent difficulty of obtaining water samples and reliable hydraulic data.

Aquitard properties, such as hydraulic conductivity, and their variability can be determined by fluid pressure measurements within the aquitard using *in situ* vibrating wire pressure transducers [6, 7], although hydraulic conductivity measurements can increase with the scale of measurement [8, 9]. When combined with the gradient of fluid pressure using Darcy's law, the vertical flow direction and rate can be determined.

Since groundwater flow velocities in aquitards can be low, mass transport in these layers tends to be dominated by molecular diffusion [2]. Spatial variations of the pore water composition have been used to evaluate the origin, age,

and migration processes of water and solutes. Complexity is introduced by climatic and hydrological changes, which are unknown with certainty at the timescales relevant to transport in aquitards, which are on the order of centuries to millions of years. Naturally occurring environmental tracers, such as chloride and stable isotopes of water, have been used in combination with mathematical models to study transport processes in aquitards and to reconstruct past environmental conditions [10].

Chloride, helium, and stable isotopes of water are considered chemically inert under a wide range of conditions. In the absence of chemical reactions, chloride is concentrated at the surface and in the unsaturated zone by evapotranspiration of rainwater. Its concentration is hence a proxy for climate and recharge rates. Similarly, stable isotopes of water form a record of climate conditions at the time of recharge as the abundance of light over heavy isotopes depends on evaporation and temperature [11]. Noble gases are good tracers of hydrogeological processes because of their inert nature and have been applied to study aquitard processes [12, 13]. Pore water noble gas compositions have been used to determine fluid sources [14], to date pore waters [15], to determine solute diffusion coefficients [16, 17] and to determine rates of water and solute mass transport [10, 13, 17–21]. Helium dissolves in the water in the unsaturated zone in equilibrium with the soil air, and its concentration in groundwater increases with age due to subsurface production, as well as upward migration of deeper crustal and mantle helium [22, 23]. Thus, while chloride and stable isotope variations can reflect changes in recharge conditions, concentrations of radiogenic helium are influenced by groundwater residence time.

Most aquitard studies have been undertaken in temperate climates, such as in Canada and Europe, where the importance of glaciation is reflected by the stable water isotopes [10, 24]. Stable isotopes of water and major element pore water profiles in shallow clay aquitards showed that solute transport is dominated by diffusion in Ontario, Canada [25], and Montreal, Canada [26]. Solute transport in surficial clay aquitards in Saskatchewan, Canada, was investigated by $\delta^{18}O$ [27], $\delta^{2}H$ [28, 29], or both [30, 31]. $\delta^{18}O$ data constrained hydraulic conductivities in these aquitards and showed diffusion to be the dominant solute transport mechanism even during glaciations [27, 30]. $\delta^{2}H$ profiles provided the timing of climate change during the Holocene [28, 29]. Stable isotopes and solute pore water distributions were used to determine transport and geochemical processes controlling pore water composition in the Battleford Formation in Saskatchewan, Canada [32], and Michigan Basin in Ontario, Canada [33].

In southwestern Spain, Konikow and Arévalo [34] were able to determine that an 80 m thick clay aquitard is in steady state with upward flow between 1 mm/yr and 1 cm/yr. Mazurek et al. [10] compiled stable isotopes of water and solute pore water profiles for nine sites in central Europe from a number of published studies [17, 35–40]. A selection of anion concentration data and stable isotopes of water as well as noble gases comprised the dataset at each site. As found in previous studies [41, 42], model scenarios confirmed that diffusion is the dominant solute transport process. A study undertaken in the Otway Basin, located in a temperate climate zone of Australia, used stable isotopes of water and major ion concentration profiles to investigate diffusive transport in an aquitard [43, 44]. Here, geochemical processes were found to complicate interpretations based on nonconservative major ions [43].

All the above studies have been undertaken in cold or temperate climates. In arid regions the residence times of water in aquifers, not just aquitards, tend to be large ($>10^4$ years) due to low recharge rates [45]. Harrington et al. [24] undertook one of the few studies in arid central Australia and used both chloride and stable isotopes of water to determine the palaeohydrogeology of the western Great Artesian Basin (GAB). The chloride profile showed a complex history of climate variations. It was found that pore water isotope contents were not as well suited to identify climate influences. This is because in arid regions and at low latitudes, their interpretation is complicated because the effects of ice volume, temperature, precipitation amount, and moisture transport on isotopic abundances in recharge are all important, whereas in study areas at higher latitudes the temperature effect due to glaciations dominates [25, 27–31]. Gardner et al. [46] used ^{4}He concentrations in the same aquitard profiles, augmented with regional groundwater samples, to estimate vertical fluid flux through the aquitard. Hasegawa et al. [47] also characterised solute transport in the main confining layer of the GAB using chloride and chlorine isotopes (^{36}Cl, ^{37}Cl) finding that Cl is of meteoric origin and is transported by diffusion. Jones et al. [48] concluded, based on vertical profiles of salinity and stable water isotopes across the Geera Clay in the Murray River Basin, that the major part of dissolved salts in the pore water was derived from aerosols.

In this study, we examine vertical groundwater flow and solute transport through an aquitard separating the GAB and the underlying Arckaringa Basin. The aquitard of interest is situated between two aquifers with long residence times of water, due to the low recharge rates in the arid climate [49]. Chloride, ^{4}He, and stable isotopes of water in conjunction with numerical and analytical modelling were used to quantify flow velocities and establish the connectivity between the two basins at the site studied.

2. Study Area

The Arckaringa Basin is a Late Carboniferous to Early Permian sedimentary basin. Glacial scouring during the Devonian-Carboniferous and faulting during the Early Permian resulted in the formation of troughs and subbasins [54]. The Boorthanna Formation, which forms the deeper aquifer (called lower aquifer in this work), is a marine and glacial sandstone and diamictite aquifer that overlies Proterozoic basement rock [55] (Figure 1(c)). The aquitard is formed by the Stuart Range Formation. It consists of mudstone, siltstone, and shale and separates the Boorthanna Formation from the overlying GAB (Figure 1(c)). The GAB sediments were deposited from the late Jurassic to the early Cretaceous [56–58]. The J-aquifer of the GAB (called the upper aquifer in this work) comprises the hydraulically connected Jurassic Cadna-owie Formation and Algebuckina Sandstone. These are confined by the outcropping Cretaceous Bulldog Shale

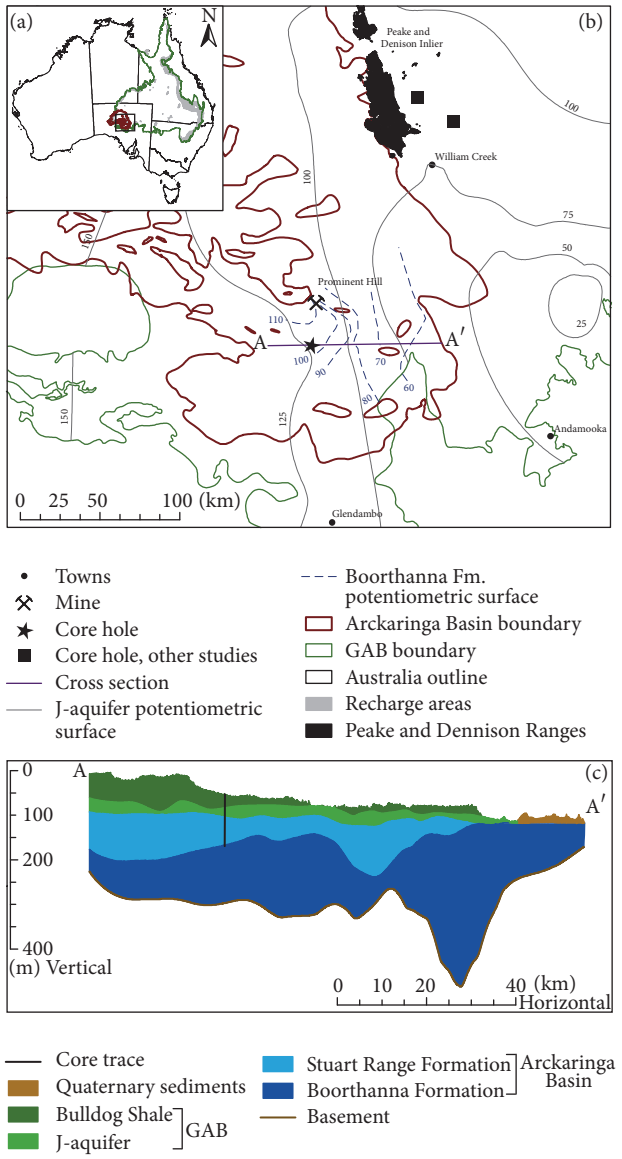

Figure 1: (a) Study location in the GAB and Arckaringa Basin in central Australia, also showing main recharge areas. (b) Location of core from this study as well as those from Gardner et al. [46] and Harrington et al. [24]. Groundwater potentiometric surfaces included with water level in m AHD. (c) Cross section showing stratigraphy and depth of the core.

[59], a marine mudstone and silt aquitard, which formed due to sea level rise at the start of the late Cretaceous [56]. Since their formation, the basins have undergone many phases of compression, uplift, and erosion to today's levels [58].

The thickness values of the Boorthanna Formation, the Stuart Range Formation, and the J-aquifer where the core is located are 131 m, 574 m, and 29 m, respectively. The Arckaringa Basin is bordered by a series of ranges, ridges, and plateaus including the Peake and Denison Inlier to the east consisting of outcropping basement rocks with an elevation of 400–420 m above Australian Height Datum (AHD) [60]. For this study, a continuous core was drilled through the Stuart Range Formation in central South Australia (Figure 1(b)). The topography of the region where the aquitard core was taken is relatively flat with an elevation of approximately 150 m AHD. It is characterised by wide flat-topped plateaus, with sharp escarpments, and lower lying gibber and flood plains associated with ephemeral rivers.

The climate is arid with an average annual precipitation rate of 120 mm/yr [61, 62]. However, precipitation is variable, both temporally and spatially. Recharge from rainfall is diffused via infiltration into outcropping and subcropping aquifer sediments (Figure 1(a)) and focused along disconnected ephemeral rivers [59, 63]. Vertical groundwater flow from the upper aquifer to the lower aquifer is likely to be the main form of recharge to the latter because it crops out only in a small area [63]. The regional groundwater flow direction in both aquifers near the coring location of this study is approximately from west to east (Figure 1(b)), although the spatial coverage of bores completed in the lower aquifer is limited. Water levels in the Boorthanna Formation range from 110 to 60 m AHD and in the J-aquifer range from 150 to 25 m AHD (Figure 1(b)). Groundwater is being extracted from the upper aquifer for stock and domestic use. The Prominent Hill mine (Figure 1(b)) has been extracting groundwater at a rate of up to 26 ML/d from the lower aquifer from wells surrounding and to the northeast of the coring location since 2008 to sustain its mining operations, which has caused drawdowns of up to 50 m [64].

3. Methodology

3.1. Sampling and Analytical Methods. The core through the GAB and the Stuart Range Formation and into the lower aquifer was drilled in March 2015. The core was drilled 30 m from existing groundwater wells completed in the J-aquifer in the GAB above the aquitard and the Boorthanna Formation in the Arckaringa Basin below [53]. Upon completion of the borehole, Vibrating Wire Piezometers (VWP) were grouted into the borehole spaced 13 m apart from 50.8 to 102.8 m through the aquitard [53]. VWP pore pressure readings were used to determine the vertical fluid pressure gradient [7].

Core samples were collected for physical and chemical analysis by first shaving off and discarding the outer core (approximately 2 mm) to avoid drilling fluid contamination. The drilling fluid had been spiked with heavy water (D_2O) to be able to confirm this. Samples for chloride and uranium/thorium analysis were collected at 2 and 5 m intervals, respectively. The 20 cm length shaved samples were vacuum-sealed in two Food Saver® bags. The $\delta^{18}O$ and $\delta^{2}H$ 5 cm length samples collected every 2 m were sealed in a small Ziploc® bag with all the air squeezed out then placed in a second large Ziploc bag following the method outlined by Wassenaar et al. [65]. Undisturbed 25 cm length samples for permeability and porosity determination were collected every 10 m and where there was a lithological change. Samples were wrapped in plastic, labelled with the depth interval and an arrow to indicate direction to top of core, then placed in a PVC pipe for protection, and vacuum-sealed in a Food Saver bag.

Samples for noble gas analysis were subcored every 5 m using a 35 mm diameter handheld electric drill, to avoid sampling the outer core that may have already degassed or been

contaminated. The subcores were immediately transferred into stainless steel canisters for storage, following the subcore degassing method developed by Osenbrück et al. [15]. After the subcores were transferred, the canisters were flushed with ultra high purity nitrogen and subsequently evacuated three times to remove any atmospheric gases [16], and the samples were then allowed to degas for 6 months before analysis.

The nearby groundwater monitoring wells screened in the upper and lower aquifers were sampled for major elements and noble gases. Major element samples were filtered with a 0.45 μm filter and collected in a rinsed HDPE bottle. Noble gas water samples were collected in copper tubes using stainless steel pinch-off clamps [66, 67].

Groundwater chloride concentrations were measured by ion chromatography by CSIRO, Adelaide, Australia, using APHA method 4110 that has a coefficient of variation <2% [68]. Uranium and thorium concentrations in the sediment samples were analysed by hydrofluoric acid digestion of the dried sediment and then analysed by mass spectrometry at the same laboratory. Noble gas groundwater concentrations were analysed by mass spectrometry in the noble gas laboratory of ETH Zurich, Switzerland, according to the methods discussed by Beyerle et al. [66]. Measurement precision is <1.0% for helium concentration.

Analysis of chloride, as well as δ^{18}O and δ^{2}H in the core pore waters and drilling fluid, was undertaken at Flinders University, Australia. It was not possible to obtain a large enough pore water sample from the core by squeezing or centrifuging. Instead, for chloride analysis, pore waters were extracted using the 1 : 5 dilution method outlined by Sacchi et al. [69]. The extracted water was filtered using a 0.45 μm filter and chloride was then analysed on a Metrohm 883 Basic IC plus ion chromatograph (IC) using in-house standard solutions to generate calibration graphs following standard analytical techniques [68]. Precision for anion analysis is ≤2.5%. δ^{18}O and δ^{2}H were analysed on a Picarro L21302-i using the vapour equilibration method outlined in Wassenaar et al. [65]. The difference between repeated measurements for δ^{18}O and δ^{2}H was ≤5%.

Conversion of the chloride concentrations obtained with the 1 : 5 dilution method into the *in situ* chloride concentration per litre of pore water is based on the so-called geochemical porosity [70–72]. The geochemical porosity (also referred to as effective porosity n_e) is less than the total porosity (n), especially for anions, which are repelled from the double layer that occupies the pore space near negatively charged minerals [71–73]. Typical experimentally derived n_e/n values range between 0.3 and 0.6, but at high ionic strength ($I \geq 1$ mol/kg) n_e can approach n as the double layer collapses [73]. The measured concentrations of solutes in the 1 : 5 dilution extract aqueous leach solution were converted to the pore water concentration (C_{geochem}) according to

$$C_R = C_L \frac{V_L}{M_R},$$
$$C_{\text{geochem}} = C_R \rho \frac{1}{n_e}, \tag{1}$$

where C_R is the mass of chloride per mass of bulk rock sample [M/M], C_L is the mass of chloride per volume of leach solution [M/L^3], V_L is the volume of leach solution [L^3], M_R is the mass of bulk sample leached [M], ρ is the bulk density [M/L^3], and n_e is the geochemical porosity [72, 74]. For chloride, n_e is estimated from n by assuming an n_e/n value of 0.7 because of the ionic strength (up to 0.7 mol/kg) of the pore waters [73].

Permeability, porosity, and moisture content measurements were undertaken by the Ground Science Engineering testing laboratory, in Victoria, Australia. The permeability of the sample was measured using a triaxial cell at the *in situ* pressure of the sample, following the method AS 1289.6.7.1-2000 [75]. The porosity of the samples was measured using both the specific gravity and bulk density (method AS 1289.5.1.1-2000) as well as the moisture content (method AS 1289.2.1.1-2000) [75]. The specific gravity test determines the density of the particles making up the sample, while the bulk density gives the volume and mass of the material. From these it is possible to determine the porosity of the sample using the method AS 1289.6.7.3-1999 [76].

The noble gases of the aquitard pore waters were determined by mass spectrometry using standard procedures [16, 77] in the facilities at Lamont-Doherty Earth Observatory, New York, US. Measurement precision is between 1.0 and 3.0% for noble gas concentrations. Some core samples were reanalysed after two weeks to ensure total degassing of the core pore fluids. Pore water concentrations were calculated using an n_e/n ratio of 1.0 since noble gases are chemically neutral and should not be affected by clay mineral double-diffusive layer charge repulsion [46].

To remove the atmospheric helium component, the concentration of neon in water in equilibrium with the atmosphere at 25°C and elevation of 150 m AHD was removed from the measured helium concentrations [23, 78]. This assumes that helium and neon are in equilibrium with the atmosphere, which is an underestimate, as it does not account for the unknown excess air component. The excess air component could not be calculated because of gas loss during sampling [15].

3.2. Modelling. Modelling was aimed at evaluating the effective ^{4}He and chloride diffusion coefficients, the internal ^{4}He release rate from solids, and the advective vertical flow component at the site. A steady state analytical solution to the 1D advection-dispersion equation developed by Solomon et al. [52] and a 1D transient numerical model using MT3DMS [51] were employed to simulate the observed helium and chloride concentrations at the site.

The 1D advection-dispersion equation (also referred to as 1D advection-diffusion equation) is

$$n_e \frac{\partial C}{\partial t} = \frac{\partial}{\partial z}\left(n_e D \frac{\partial C}{\partial z}\right) - \frac{\partial}{\partial z}\left(v_z n_e C\right) + n_e \rho G, \tag{2}$$

where v_z is linear pore water velocity [L/T], C is the concentration of chloride [M/L^3] or helium [L^3/L^3] in pore water, z is the vertical spatial coordinate (positive downward) [L], D is the coefficient of hydrodynamic dispersion [L^{2}T^{-1}], n_e is the effective porosity, that is, the porosity accessible to the solute, G is accumulation rate per mass of pore water due to zero-order production, that is, radiogenic ^{4}He accumulation

rate per volume of pore water [L^3/L^3T] ($G = 0$ for Cl), ρ is water density [M/L^3], and t is time [T].

Under steady state conditions, the transport of a solute that is being produced in the subsurface at a constant rate is described by the following equation:

$$v_z \frac{\partial C}{\partial z} = D\frac{\partial^2 C}{\partial z^2} + \frac{G^*}{n_e}, \quad (3)$$

where G^* is the release rate per volume of sediment due to zero-order production, that is, radiogenic ^{4}He accumulation rate per volume of sediment [L^3/L^3T] ($G^* = 0$ for Cl).

The analytical solution of (2), subject to boundary conditions, is given by Solomon et al. [52] as

$$C(z) = \frac{C_L - G^* L/v_z n_e}{1 - \exp(v_z L/D)} \left\{1 - \exp\left(\frac{v_z z}{D}\right)\right\} + \frac{G^* z}{v_z n_e}, \quad (4)$$

where L is the depth from the top of the aquitard to the bottom of the aquitard [L] and G^* is the release rate per volume of sediment [L^3/L^3T].

For low advection velocities, the coefficient of hydrodynamic dispersion (D) is simplified to the effective diffusion coefficient (D_e) as the contribution of hydrodynamic dispersion to D becomes insignificant. The effective diffusion coefficient can be estimated using an Archie's Law relationship [79]:

$$D_e = D_o n_e^m, \quad (5)$$

where D_o is the free solution aqueous diffusion coefficient ($D_o = 6.40 \times 10^{-2}$ m^2/yr for chloride at 25°C and $D_o = 2.30 \times 10^{-1}$ m^2/yr for ^{4}He at 25°C) [80–82] and m is an empirical exponent known as the cementation factor. For anions, m = 2–2.5 based on laboratory measurements, so a value of 2.3 was used for chloride, as per Harrington et al. [24]. As helium has access to the same pore volume as water, $m = 2$ was selected for ^{4}He to obtain the maximum expected diffusion coefficient [10, 46]. An average measured *in situ* temperature of 25.4°C (range 24.9–26.0°C; Table 1) measured via the VWP thermistors meant that D_e values did not need to be temperature corrected.

The radiogenic ^{4}He release rate from sediment in cm^{3}STP/m$^3_{\text{rock}}$/yr (G^*) can be calculated with

$$G^* = 0.2355 \times 10^{-12}\left([U]\left(1 + 0.123\left(\frac{[Th]}{[U]} - 4\right)\right)\right)(\rho \Lambda_{\text{He}}). \quad (6)$$

And the radiogenic ^{4}He accumulation rate per volume of pore water in cm^{3}STP/m$^3_{\text{H}_2\text{O}}$/yr (G), assuming water density = 10^6 g/m^3, can be calculated with [23, 83]

$$G = G^*\left(\frac{1-n}{n}\right), \quad (7)$$

where $\Lambda_{\text{He}} = 1$ [22], ρ is the density of the sediment and water filled pore spaces [M/L^3], and [U] and [Th] are the concentrations of uranium and thorium expressed in parts per million.

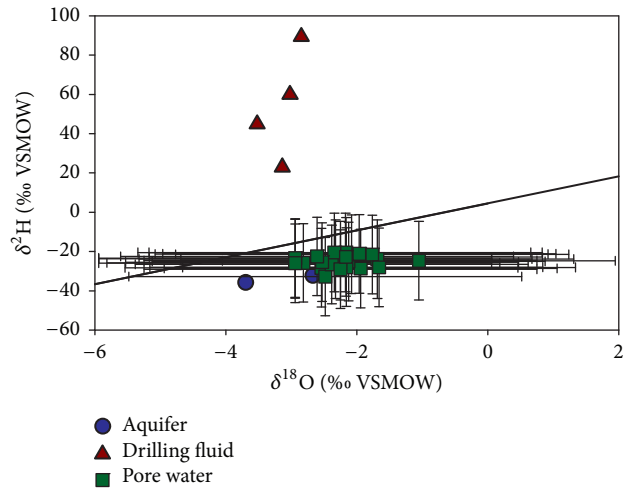

FIGURE 2: δ^{18}O and δ^2H in pore water, groundwater, and drilling fluid samples. Error bars represent the possible isotopic equilibrium fractionation difference for samples with less than 3 g water adapted from Hendry et al. [50]. The black line represents the local meteoric water line (LMWL), $\delta^2\text{H} = 7.2\delta^{18}\text{O} + 5.7$, from Alice Springs.

The relative importance of advection and diffusion in an aquitard of thickness L can be characterised by the Peclet number (Pe). Neglecting dispersion and accounting for the effective porosity (n_e) under steady state boundary conditions, Pe is defined as [84]

$$\text{Pe} = \frac{v_z L}{n_e D_e}. \quad (8)$$

Values of Pe <1 indicate that transport over distance L is dominated by diffusion, whereas if Pe >1, then advection will be dominant over diffusion.

Model parameters and boundary conditions are listed in Table 2. The same boundary conditions were used in both the analytical solution and the MT3DMS numerical model. The solute profiles were simulated over the entire aquitard sequence, that is, extending from 46.6 metres below the surface at the top boundary to 104 metres below the surface at the base. The vertical linear pore water velocity (v_z) was fixed, and hydraulic parameters such as hydraulic conductivity (K_V) and porosity (n) were held constant in all simulations assuming steady state flow conditions in the aquitard. Upper and lower boundary concentrations were fixed in the models (Dirichlet type), but the solute concentrations could be variable in time in the transient MT3DMS numerical model. The radiogenic ^{4}He accumulation rate (G) was also fixed as this was calculated from U and Th concentrations measured in four aquitard samples (Table 1).

4. Results

4.1. Field Data. The measured groundwater and pore water compositional data and hydraulic properties are given in Table 1. The δ^2H values of the pore waters (from −20 to −33‰ VSMOW) are higher compared to the groundwater samples (from −32 to −36‰ VSMOW; Figure 2). Likewise, the δ^{18}O values of the pore waters (from −1.1 to −2.9‰ VSMOW)

Table 1: Aquitard pore water chemistry, measured aquitard properties, groundwater chemistry in italics, and uranium and thorium concentrations in sediment samples.

Formation	Depth (m)	Elevation (m AHD)	Water Level (m AHD)	Temperature °C	Hydraulic conductivity - K_V (m/yr)	Density - ρ (g/cm^3)	Porosity - n (% vol)	Moisture content (%)	Thorium (mg/kg)	Uranium (mg/kg)	^{4}He (ccSTP/g_{H_2O})	Ne (ccSTP/g_{H_2O})	Ar (ccSTP/g_{H_2O})	Cl (mg/L)	δ^2H (‰ VSMOW)	δ^{18}O (‰ VSMOW)
Bulldog Shale (aquitard)	0.00	154.00														
	10.80	143.20			6.31×10^{-3}	1.65	58.10	48								
Upper aquifer (J-aquifer)	17.80	136.20														
	34.55	119.45			$1.89 \times 10^{+1}$	1.80	42.80	19	2.32	0.96						
	39.00	115.00	*114.96*	25.2					1.12	1.08	*8.70×10^{-8}*	*1.87×10^{-7}*	*2.61×10^{-4}*	*6390*	*−32.2*	*−2.7*
	46.60	107.40			3.15×10^{-1}	2.40	13.30	5								
Stuart Range Formation (aquitard)	46.60	107.40														
	47.23	106.78							1.12	1.08				6302	−28.7	−1.9
	48.33	105.68			3.15×10^{-4}	2.21	26.00	11							−23.9	−1.7
	48.68	105.33												6053		
	50.68	103.33	109.65	24.89							1.17×10^{-6}	1.16×10^{-7}	2.02×10^{-4}	5532	−21.5	−1.8
	52.23	101.78												6029	−21.3	−2.1
	53.70	100.30			2.52×10^{-4}	2.26	25.00	11								
	55.58	98.43									3.08×10^{-6}	1.34×10^{-7}	2.09×10^{-4}	5416	−25.0	−2.1
	56.73	97.28												5222		
	58.60	95.40			6.31×10^{-5}	2.26	24.70	11	1.21	1.23						
	59.73	94.28												5466	−23.9	−2.3
	61.13	92.88									5.73×10^{-6}	1.28×10^{-7}	2.11×10^{-4}	5472	−28.1	−1.7
	62.63	91.38	108.73	24.92										5237	−20.5	−2.2
	66.38	87.63												4518	−28.2	−2.5
	68.00	86.00												5226	−24.6	−2.2
	68.30	85.70			1.26×10^{-2}	2.31	21.90	10								
	69.73	84.28									9.38×10^{-6}	1.24×10^{-7}	2.09×10^{-4}			
	71.25	82.75												6909	−32.8	−2.5
	73.15	80.85									9.65×10^{-6}	1.70×10^{-6}	1.02×10^{-3}	5658	−26.6	−2.4
	76.15	77.85	106.44	25.36										5955	−24.7	−1.1
	77.30	76.70			1.89×10^{-5}	2.32	20.70	9								
	78.20	75.80									1.20×10^{-5}	1.59×10^{-7}	2.00×10^{-4}	6142	−28.0	−2.2
	80.65	73.35												6192	−29.0	−2.3
	83.15	70.85												6886	−20.5	−2.3
	84.20	69.80			1.26×10^{-5}	2.33	20.40	8			1.75×10^{-5}	1.13×10^{-7}	1.97×10^{-4}			
	85.45	68.55												8008	−23.7	−2.9
	87.08	66.93							0.79	2.31				9173	−25.8	−2.8
	90.48	63.53	105.01	25.7												
	90.60	63.40									1.81×10^{-5}	4.29×10^{-6}	1.68×10^{-3}	14439	−25.4	−2.5
	91.78	62.23			6.31×10^{-5}	2.49	12.10	4								
	93.15	60.85												10548	−22.5	−2.6
	95.23	58.78												12001	−23.3	−2.9
	97.30	56.70									2.10×10^{-5}	1.17×10^{-7}	1.83×10^{-4}	15087	−21.2	−2.0
	99.25	54.75			2.21×10^{-4}	2.27	22.30	11								
	99.73	54.28												14469	−25.9	−2.9
	102.08	51.93	103.33	25.96										14347	−22.7	−2.2
	103.73	50.28									2.94×10^{-5}	1.11×10^{-7}	1.95×10^{-4}			
	103.88	50.13							2.07	1.68				16564		
Lower aquifer (Boorthanna Formation)	104.00	50.00														
	106.73	47.28							2.64	1.76						
	108.00	46.00	*107.74*	27.44	1.58×10^{-4}	2.31	20.10	8.1			*7.99×10^{-5}*	*1.98×10^{-7}*	*2.64×10^{-4}*	*21500*	*−35.8*	*−3.7*
	138.00	16.00														

Table 2: Solute transport model boundary conditions and scaled root mean squared error (SRMS). The model parameters determined from the aquitard core samples are bold, whereas the nonbold model parameters were allowed to vary from those calculated and estimated from the aquitard core measurements to improve model fit with measured pore water concentrations.

	K_V (m/yr)	v_z (m/yr)	G (ccSTP/m$^3_{H_2O}$/yr)[a]	Solute	D_e (m^2/yr)[b]	n_e	Upper boundary			Lower boundary		SRMS ^{4}He	SRMS Cl
							C_i[c]	C t = 0 yrs	C t > 417,000 yrs	C_i[c]	C t = 3000 yrs		
Model 1 (diffusion only)[d]	0	0	$\mathbf{2.1 \times 10^{-6}}$	Chloride	$\mathbf{1.9 \times 10^{-3}}$	0.182	5200			21500		37	38
				^{4}He	$\mathbf{1.1 \times 10^{-2}}$	0.216	8.7×10^{-8}			8.0×10^{-5}			
Model 2 (calculated boundary conditions)	$\mathbf{4.6 \times 10^{-5}}$	$\mathbf{2.3 \times 10^{-5}}$	$\mathbf{2.1 \times 10^{-6}}$	Chloride	$\mathbf{1.9 \times 10^{-3}}$	0.182	5000			21500		37	36
				^{4}He	$\mathbf{1.1 \times 10^{-2}}$	0.216	8.7×10^{-8}			8.0×10^{-5}			
Model 3 (optimised boundary conditions)	4.3×10^{-4}	3.5×10^{-4}	$\mathbf{2.1 \times 10^{-6}}$	Chloride	7.8×10^{-4}	0.182	5000			21500		20	12
				^{4}He	1.2×10^{-3}	0.216	8.7×10^{-8}			8.0×10^{-5}			
Model 4 (model 3 - time to steady state)	4.5×10^{-4}	3.5×10^{-4}	$\mathbf{2.1 \times 10^{-6}}$	Chloride	7.8×10^{-4}	0.182	21500[e]	5000[f]	—	21500	—	20	12
				^{4}He	1.2×10^{-3}	0.216	8.0×10^{-5}[e]	8.7×10^{-8}[f]	—	8.0×10^{-5}	—		
Model 5 (model 3 -chloride increase)	4.5×10^{-4}	3.5×10^{-4}	$\mathbf{2.1 \times 10^{-6}}$	Chloride	7.8×10^{-4}	0.182	21500[e]	5000[f]	6390[g]	21500	—	20	10
				^{4}He	1.2×10^{-3}	0.216	8.0×10^{-5}[e]	8.7×10^{-8}[f]	—	8.0×10^{-5}	—		
Model 6 (reduced concentrations)	8.6×10^{-4}	7.0×10^{-4}	$\mathbf{2.1 \times 10^{-6}}$	Chloride	$\mathbf{1.9 \times 10^{-3}}$	0.182	5000			16600[h]		18	12
				^{4}He	$\mathbf{1.1 \times 10^{-2}}$	0.216	8.7×10^{-8}			3.0×10^{-5}[h]			
Model 7 (model 6 - groundwater extraction)	8.6×10^{-4}	7.0×10^{-4}	$\mathbf{2.1 \times 10^{-6}}$	Chloride	$\mathbf{1.9 \times 10^{-3}}$	0.182	5000	6390	—	16600	21500[i]	6	10
				^{4}He	$\mathbf{1.1 \times 10^{-2}}$	0.216	8.7×10^{-8}	—	—	3.0×10^{-5}	8.0×10^{-5}[i]		

[a] $G = G^*((1-n)/n)$, so $G^* = 5.5 \times 10^{-7}$ ccSTP/m$^3_{aq}$/yr. [b] Closer inspection of the equations used in MT3DMS [24, 51], and the steady state solution [20, 52] reveals the effective diffusion coefficient input parameter is actually equivalent to D_p, where $D_p = D_e/n_e$. [c] Chloride concentration units are mg/L and helium concentrations units are ccSTP/g$_{H_2O}$. [d] Model 1 run in MT3DMS as v_z cannot equal zero in the steady state solute transport analytical solution due to the development of the solution. [e] High initial concentration to represent possible initial conditions. [f] Instantaneous reduction (freshwater flushing) to estimate minimum time required to reach steady state solute transport. [g] Instantaneous chloride concentration increase (increased evapotranspiration) to give the minimum time required to match upper profile. [h] Reduced chloride and helium concentrations in the lower boundary to give best steady state solute transport profile fit. [i] Instantaneous increase in lower boundary concentrations as a result of groundwater extraction.

Table 3: Measured aquitard core properties bolded [53] and calculated vertical flow velocities, diffusion coefficients, geochemical porosity, and Peclet numbers for ^{4}He and in brackets for chloride.

	min K_V	max K_V	Mean K_V
K_V (m/yr)	$\mathbf{1.3 \times 10^{-5}}$	$\mathbf{1.3 \times 10^{-2}}$	$\mathbf{4.6 \times 10^{-5}}$
v_z (m/yr)	6.0×10^{-6}	6.5×10^{-3}	2.3×10^{-5}
n_e		0.216 (0.182)[a]	
D_e (m^2/yr)		1.1×10^{-2} (1.9×10^{-3})[b]	
Thickness of aquitard (m)		57.4	
Peclet numbers	0.1 (1)[c]	160 (1082)[c]	1 (4)[c]

[a]Lower effective porosity for chloride in brackets. [b]Smaller effective diffusion coefficient for chloride in brackets. [c]Peclet number for chloride in brackets.

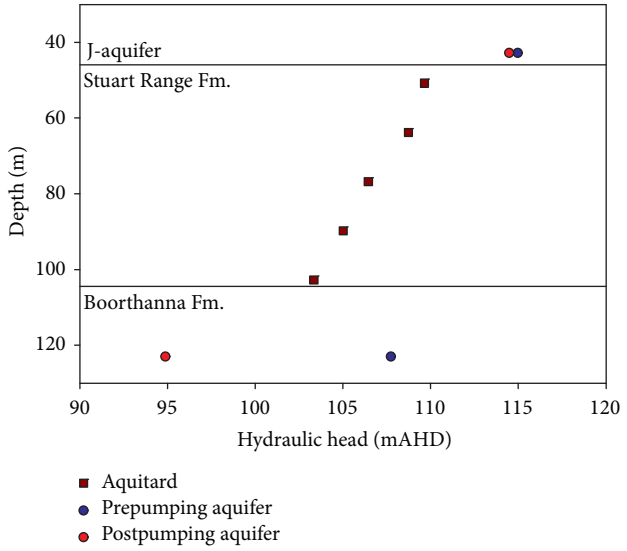

Figure 3: Hydraulic head in m AHD by the VWP installed throughout the aquitard and measured in nearby wells in the upper aquifer and lower aquifer.

are higher than the groundwater samples (from −2.7 to −3.7‰ VSMOW; Figure 2). Even though the samples had more than 5% moisture content (Table 1) required for the applied method [65], it is possible that there was insufficient sample collected to equilibrate with the Ziploc bag headspace. Hendry et al. [50] determined that samples with less than 3 g of water appear more enriched due to isotope fractionation by water loss to the bag headspace. Contamination by the deuterium spiked drilling fluid would cause enrichment in δ^2H composition only. The slight enrichment of both δ^2H and δ^{18}O in the pore water compared to the groundwater samples is therefore believed to be due to insufficient pore water in the bag rather than drilling fluid contamination during sampling (Figure 2). Because of the suspected analytical problems and the large relative errors (Figure 2), the pore water isotopes results were not further considered for modelling.

The measured vertical hydraulic conductivity (K_V) of the aquitard ranges from 1.3×10^{-5} to 1.3×10^{-2} m/yr while porosity ranges from 0.12 to 0.26 with no discernible pattern with depth (Table 1). The VWP data and hydraulic head measurements in the aquifer piezometers indicate downward flow (Figure 3). Pumping from the lower aquifer since 2008 has affected the current flow system by increasing the hydraulic head difference between the upper aquifer and lower aquifer (Figure 3). Calculation of the vertical groundwater flow rate using Darcy's law and the harmonic mean K_V of 4.6×10^{-5} m/yr and porosity of 0.216 (Table 3) [53] and prepumping freshwater heads, measured prior to the onset of pumping by Prominent Hill mine, give a vertical linear pore water velocity (v_z) of 2.3×10^{-5} m/yr (range of 6.0×10^{-6}–6.5×10^{-3} m/yr; Table 3). Thus, Pe could range from 0.1 to 160 for ^{4}He and from 1 to 1082 for chloride (Table 3). The range of Pe values indicates that solute transport in the system could be driven by diffusion, advection, or both depending on which K_V measurement is representative of the aquitard as a whole.

Pore water chloride and helium profiles are presented in Figure 4. Chloride pore water concentrations range from 4,518 to 16,564 mg/L (Table 1) [73]. The lowest chloride concentrations occur around a depth of 65 m. The increase in chloride concentration at the top of the profile suggests there has been a change in the upper boundary condition.

The ^{4}He pore water concentrations with the atmospheric component removed using the concentration of neon in water in equilibrium with the atmosphere at 25°C and elevation of 150 m AHD range from 1.2×10^{-6} to 2.9×10^{-5} ccSTP/g_{H_2O} (Table 1). Neon concentrations in all but two pore water samples are approximately 14–39% less than the values expected for atmospheric equilibrium. This is consistent with Osenbrück et al. [15] who estimated the gas loss during vacuum extraction to be approximately 30% of the total gas in the pore water. This has been incorporated in the ^{4}He concentration uncertainty range, indicated by the bars in Figure 4(b). The remaining two pore water samples showed a neon excess greater than 30%, with Ar/Ne ratios between $4 \times 10^{+2}$ and $6 \times 10^{+2}$ showing that the excess is caused by atmospheric air contamination (Ar/Ne = $5 \times 10^{+2}$). The amount of air contamination required to explain the neon and argon concentration was calculated [78] and removed from the helium pore water concentrations to obtain the terrigenic and *in situ* helium production components (Table 1). The above corrections and the assumptions therein make very little difference as the pore water ^{4}He concentrations are >2500% of the atmospheric ^{4}He concentrations. The ^{4}He pore water concentrations follow a linear trend with depth. The groundwater sample from the lower aquifer has an almost three-time larger concentration than the deepest pore water sample

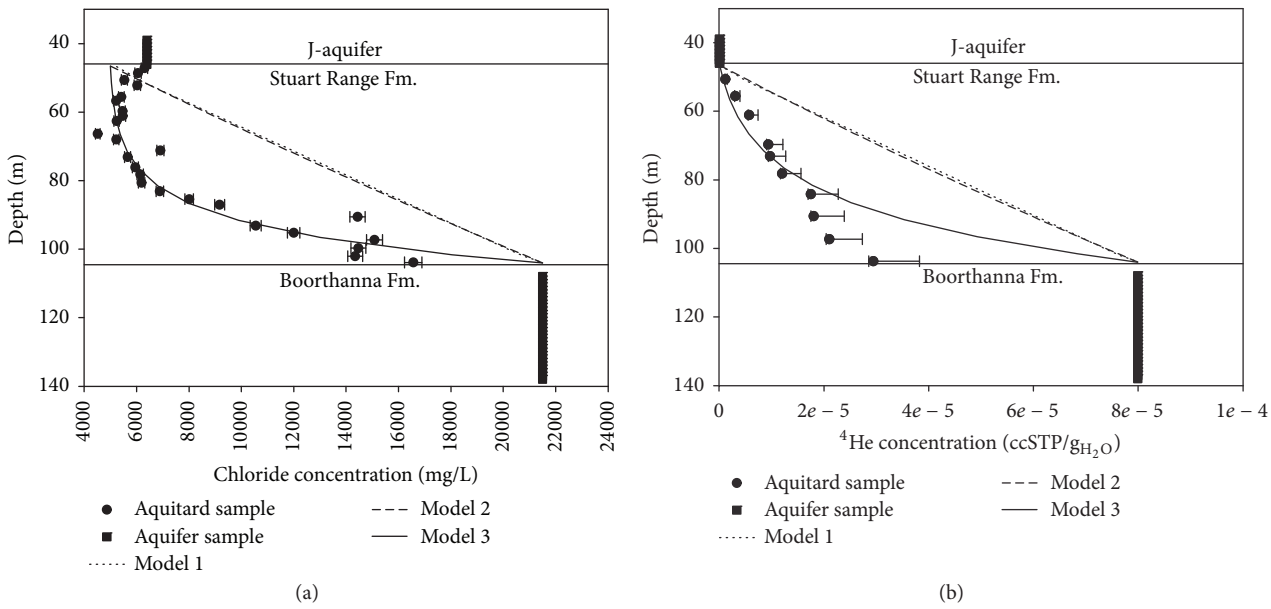

Figure 4: Profiles of (a) chloride and (b) ^{4}He concentrations. Circles indicate the pore water concentrations and the vertical bar represents the concentration in the aquifer, where the vertical length represents the screened interval. Error bars include total field, analytical errors, and, for ^{4}He, the 30% degassing loss during vacuum extraction (could be as high as 50% according to difference between measured and estimated Ne concentrations). The dotted line represents steady state solute transport analytical model 1 using estimated and calculated boundary conditions from our core measurements but diffusion-only solute transport. The dashed line represents the steady state solute transport analytical model 2 using the estimated and calculated boundary conditions. The solid line represents the steady state solute transport analytical model 3 calibration of boundary conditions (v_z and D_e).

(Figure 4(b)) and is thus clearly offset from the linear trend within the aquitard.

4.2. Model Scenarios. The vertical hydraulic gradient through the aquitard (0.12) is three orders of magnitude greater than the horizontal hydraulic gradient in the aquifers (<0.0008; Figure 1) so one-dimensional vertical flow and transport simulations are considered appropriate for the solute profiles. Long groundwater flow paths in both aquifers and long-term stability in water chemistry associated with these may justify constant concentration boundary conditions. Therefore, the first conceptual models assumed constant concentration boundary conditions for both the upper and lower aquifers, as well as steady state solute transport (Table 2). The measured ^{4}He and chloride concentrations of the aquifer samples provided constraints at the top and bottom of the aquitard. This assumes that the concentrations at the well screens were representative for those at the aquitard boundaries (i.e., homogeneous aquifer concentrations), which will be reassessed later. In the first model realisation (model 1) transport was controlled by diffusion, with advection (vertical linear pore water velocity) being zero (Table 2). In model 2, the average calculated vertical linear pore water velocity based on Darcy's law was included, while in model 3 the estimated diffusion coefficients and vertical linear pore water velocity were adjusted to optimise the fit between the model and the measured solute profiles (Table 2).

A fourth model realisation was set up in order to assess the time required to reach steady state. As initial conditions in the aquitard are unknown, it was necessary to assume that the initial chloride concentration in the aquitard pore water profile equaled the lower aquifer chloride concentration (Table 2). It is difficult to estimate the initial ^{4}He concentrations, but considering that sediments recently deposited often release excess helium that built up in sediments prior to being weathered [20], we assumed that ^{4}He concentrations are equal to the lower aquifer concentration (Table 2). Identical transport parameters as model 3 were used, where initial pore water chloride concentration of 21,000 mg/L and helium concentration of 8.0×10^{-5}ccSTP/g$_{H_2O}$ were assumed as the initial conditions (Table 2).

We hypothesise that the chloride increase visible in the upper 10 m of the profile is from reduced recharge and a subsequent increase in chloride concentration in the upper aquifer. As the flow path lag time and rate of climate change are unknown, an instantaneous concentration increase in the aquifer can estimate the minimum time since reduced recharge. This was tested in model 5 by increasing the chloride concentration in the upper boundary to the concentration measured in the upper aquifer once steady state solute transport was reached in model 4 (Table 2). Reduced recharge would also increase the ^{4}He concentration in the upper aquifer as the flow rates decrease, but since the concentrations in the aquifer are of an order of magnitude lower than that in the aquitard, this relative change is inconsequential.

In all of the above models, homogeneous solute concentrations throughout the aquifers are assumed. However, it is possible that the aquifers are chemically and isotopically

stratified [3, 85], such that the aquifer solute concentrations do not represent the top and bottom boundary conditions of the pore water profile. The helium concentration in the lower aquifer especially may not be representative because of upward diffusion from sediments below [85]. In order to test this, the lower boundary concentrations were reduced to those that fit the pore water profile in model 6 (Table 2). Model 7 tested subsequent perturbation of model 6 in the upper aquifer from reduced recharge and lower aquifer due to groundwater extraction (Table 2).

Comparison of different simulation results with measured data was undertaken using the scaled root mean squared error (SRMS) [86]:

$$\mathrm{SRMS} = \frac{100}{\Delta C}\pi\sqrt{\frac{1}{n}\sum_{i=1}^{n}\left(z_{hi} - C_i\right)^2}, \quad (9)$$

where z_{hi} are measurements of C_i at n locations and times and ΔC is the range of measured concentrations across the model domain.

Selection of the most appropriate model was based on both the SRMS errors and whether it was justifiable from a hydrogeological perspective.

The helium accumulation rate ($G = 2.1 \times 10^{-6}$ ccSTP/$m^3_{H_2O}$/yr) and porosity ($n = 0.216$) determined from the core rock samples were kept constant in the models. The diffusion coefficients, vertical linear pore water velocity estimated from current day hydraulic head measurements, or initial solute boundary concentrations were varied in models 3–7 to provide the best fit for both chloride and helium with the smallest SRMS errors, as outlined in Table 2.

4.3. Model Results. The diffusion-only transport scenario (model 1, $v_z = 0$) led to a linear concentration profile between the upper and lower aquifer (Figure 4), as expected. Model 2 differed only from model 1 in that it also included advection-driven solute transport ($v_z = 2.3 \times 10^{-5}$ m/yr; Table 2) but this resulted in only a slight adjustment in the simulated concentrations throughout the aquitard (Figure 4(a)). However, in model 3 adjustment of transport parameters ($v_z = 3.5 \times 10^{-4}$ m/yr, $D_e = 1.2 \times 10^{-3}$ m^2/yr for helium, and $D_e = 7.8 \times 10^{-4}$ m^2/yr for chloride; Table 2) provided a closer match not only for chloride, but also for the ^{4}He concentration profile (Figure 4).

The characteristic timescales for diffusion and advection are 4×10^5 years (calculated using $t = z^2/(4D_e)$) and 12×10^5 years (calculated using $t = z/v_z$), respectively. This was further investigated in model 4 to simulate freshening of the aquifers. After an instantaneous reduction in the boundary concentrations, steady state solute transport is reached after 417,000 years for chloride and 369,000 years for helium (Figures 5(a) and 5(b)). However, the assumption of a constant flow velocity, amongst other factors, over such a long time span is of course questionable. Once steady state conditions were reached in the numerical model, the chloride concentration at the upper boundary was increased to its present-day value measured in the upper aquifer in model 5 to infer the timing of the chloride concentration increase (Table 2). The simulated chloride concentration in the upper section of the profile best matched the measurements when it was assumed that the increase occurred 3000 years ago (Figures 5(c) and 5(d)).

Model 6 was used to determine if the chloride and ^{4}He concentrations could be stratified in the lower aquifer, rather than homogeneous within the aquifer. The lower boundary concentrations were reduced to those at the lower section of the pore water profile (16,600 mg/L chloride and 3.0×10^{-5} ccSTP/g_{H_2O} helium; Table 2). Except adjusting the vertical linear pore water velocity ($v_z = 7.0 \times 10^{-4}$ m/yr), all other transport parameters were the same as in model 2 (Table 2). The numerical model was then used for model 7, to increase the chloride concentration to that measured in the upper aquifer (6390 mg/L chloride; Table 2), and provides a match with the profile after 3000 years (Figure 6(c)). The increase in the lower aquifer caused by pumping was considered by increasing the helium and chloride concentration in the lower aquifer to the measured concentrations in the lower aquifer, which still matches the profile after 10 years. Model 7 provided the best fit for both chloride and helium with the smallest SRMS errors (Table 2; Figures 6(c) and 6(d)).

5. Discussion

The recent pumping has only minimally affected the aquitard solute profiles, because, with the estimated flow rate ($v_z = 6.0 \times 10^{-6}$–6.5×10^{-3} m/year; Table 3) and 10 years of pumping, solute displacement will only have been up to 6 cm. Therefore, the solute transport profiles still reflect the changes brought about by processes operating over much longer timescales.

The modelled solute concentration profiles are sensitive to the inputs D_e and v_z as well as G. Both the field measurement-based and model-optimised values fall well within the range of values reported in the literature. D_e commonly ranges from 2×10^{-2} to 2×10^{-5} m^2/yr for chloride and from 2×10^{-2} to 2×10^{-5} m^2/yr for helium [10, 16–18, 24, 46]. K_V and v_z values of 0.3×10^{-4}–3×10^{-4} m/yr and 1×10^{-3}–1×10^{-5} m/yr, respectively, have been found in previous studies [8]. The radiogenic helium accumulation rate (G) of 2.1×10^{-6} ccSTP/$m^3_{H_2O}$/yr ($G^* = 5.5 \times 10^{-7}$ ccSTP/m^3_{aq}/yr) is similar to the production rates calculated for the aquifers and aquitards of the GAB, that is, 1×10^{-5}–4×10^{-6} ccSTP/$m^3_{H_2O}$/yr, reported in other studies [22, 46, 87–89].

Steady state vertical flow conditions were assumed for all the models, although changes in recharge as well as topography over the timescales required to reach steady state conditions may have resulted in variations of the vertical flux. However, given the uncertainty about the variability of hydrogeological conditions within the aquifers, it is not possible to justifiably include any transient flow conditions in the models. Moreover, good model fits are obtained based on the steady state assumption with minor perturbations to account for transience at the aquitard boundaries.

Models 1 and 2 were unable to explain the ^{4}He and chloride solute pore water profiles (^{4}He and Cl SRMS errors >30; Table 1; Figure 4). Through calibration of the model transport parameters v_z and D_e (i.e., model 3 and model 5),

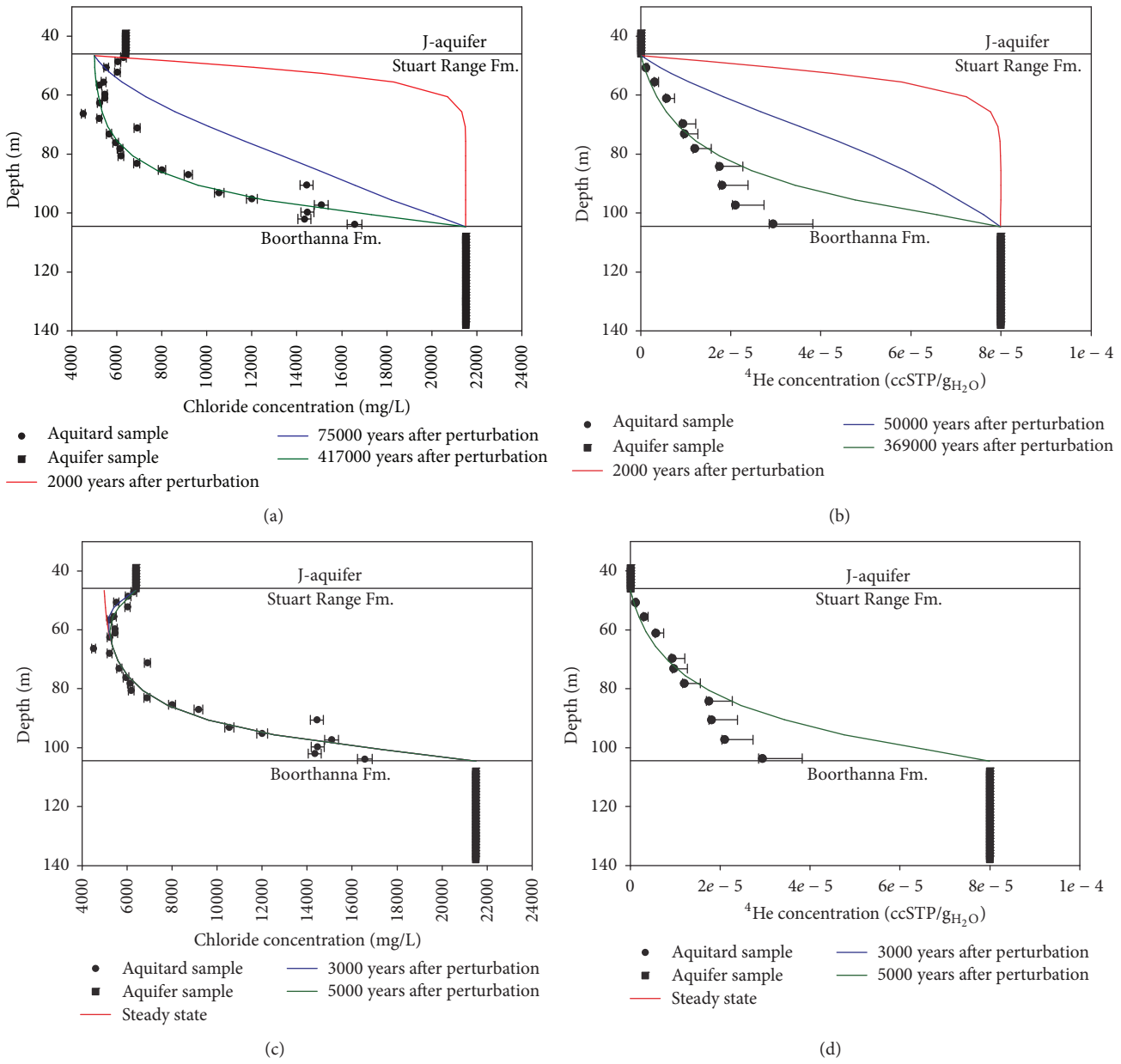

FIGURE 5: Time taken to reach steady state solute transport in model 4 from continuous high concentrations throughout the profile for (a) chloride and (b) ^{4}He concentration; the chloride concentration was then increased in the upper aquifer in model 5 giving the profiles for (c) chloride and (d) ^{4}He concentration.

a close match for the chloride concentration profile (Figures 4(a) and 5(c)) and a reasonable match for the ^{4}He concentration data were obtained (Figures 4(b) and 5(d)). Thus, model simulations suggest that the concentration profiles may largely reflect steady state conditions. Model 4 estimated that 417,000 years are needed to reach equilibrium (Figures 5(a) and 5(b)). In models 3–5 the helium diffusion coefficient ($D_e = 1.2 \times 10^{-3}$ m^2/yr) is an order of magnitude smaller than the value based on (5) and porosity ($D_e = 1.1 \times 10^{-2}$ m^2/yr). These models provided a good match for chloride (Cl SRMS error = 10; Table 2), although the SRMS error in these models' realisations was still deemed too high for helium (^{4}He SRMS error = 20; Table 2).

Model 6 provided a good fit for the helium profile (Figure 6(b); ^{4}He SRMS error = 18; Table 2). The match between the model and the measured chloride concentrations (Cl SRMS error = 12; Table 2) was good as well, except in the top part of the solute profile (Figure 6(a)). The SRMS errors (Cl SRMS error = 10; ^{4}He SRMS error = 6; Table 2) could be lowered by considering an increase in the chloride concentration since 3,000 years for chloride at the top of the aquitard, and an increase in ^{4}He and chloride at the

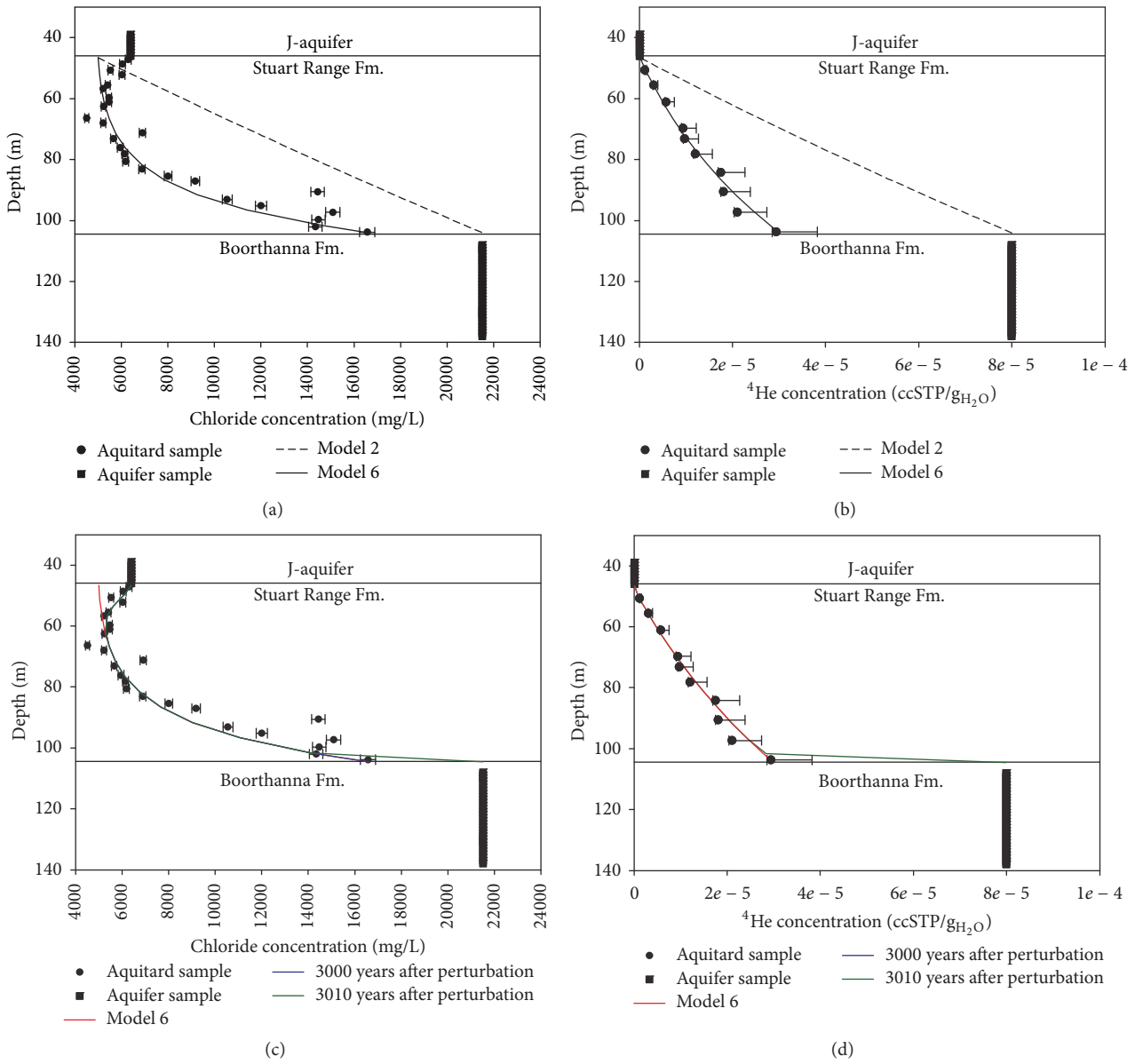

Figure 6: Steady state solute transport model 6 represented as a solid line compared to steady state solute transport analytical model 2 represented as a dashed line for (a) chloride and (b) ^{4}He concentration. The chloride concentration was then increased in the upper aquifer and then subsequently the helium and chloride concentrations were increased in the lower aquifer in model 7 giving the modelled profile for (c) chloride and (d) ^{4}He concentration.

bottom since 10 years. The model shows that the increase in concentrations in the lower aquifer has not changed the aquitard pore water profiles in the 10-year period in which concentrations have increased (Figures 6(c) and 6(d)).

The three-time larger ^{4}He concentration in the lower aquifer compared to aquitard pore waters is likely because of additional ^{4}He production and upward diffusion from the basement [85]. The ^{4}He concentration in the lower aquifer and an estimated accumulation rate of 3×10^{-5} ccSTP/m$^3_{H_2O}$/yr including upward diffusion from the basement as well as helium production (G) [90] give a groundwater residence time of >1 Ma (calculated using $t = C/G$), highlighting that groundwater flow rates are slow at the site [49]. If the water flows very slowly, the horizontal flow will not smear out the vertical solute and isotope gradients [91]. The onset of groundwater pumping by the Prominent Hill mine in 2008 most likely extracted groundwater with higher helium and chloride concentrations from the basement below or a stagnant zone. Alternatively, there could be offset due to the different sampling and measurement procedures between the aquitard and aquifer samples. The calibration of the mass spectrometers is unlikely to be the cause as the different measurement methods were undertaken with strict quality control measures. While there can be a sampling bias, it

is not possible to directly compare the methods because aquifers have relatively high permeabilities; therefore water will drain out after sample collection and the gas signal will not be retained. Additionally, an aquifer core sample is likely to be contaminated by drilling fluids. However, the authors consider the sampling and measurement procedure unlikely to be the only cause of the offset because there is no offset between the upper aquifer and upper aquitard helium measurements (Figure 4).

The chloride concentration gradient at this location with higher salinity in the lower aquifer differs from the aquitard of Harrington et al. [24] and Jones et al. [48]. The source of the dissolved salts in groundwater may be seawater, a result of evapotranspiration, a reflux brine below a discharge area, or a continental brine [11, 48, 92]. The source of the salinity in the lower aquifer is most likely not seawater as the stable water isotope delta values are representative of meteoric water (Figure 2). Moreover, the concentrations are greater than that of seawater and sea retreated 90 Ma ago. Thus, it seems highly unlikely that seawater would still be present in the pore waters. Evapotranspiration can concentrate salts up to 20 g/L [93] and could explain the chloride concentrations at this location [49]. The high salinity in the lower aquifer is also typical of those found in discharge environments elsewhere in Australia [48, 94], although it is clear that discharge does not occur at this location at present. The origin of the high salinity cannot be established with certainty, but it must have formed under hydrogeological conditions much different from those today.

Gardner et al. [46] and Harrington et al. [24] modelled the chloride and helium profiles in the surficial aquitard (Bulldog Shale) confining the upper aquifer at two locations approximately 160 km from our site (Figure 1). Gardner et al. [46] determined that helium transport through the aquitard is in steady state with an upward vertical linear pore water velocity between 5.7×10^{-3} and 3.8×10^{-6} m/yr. This magnitude is comparable with our modelled vertical linear pore water velocity of 7.0×10^{-4} m/yr, albeit the fact that the direction is opposite. The chloride profiles in Harrington et al. [24] reflect varying chloride inputs from the surface due to palaeoclimate changes. An increase in chloride concentration in the upper aquifer was interpreted to have occurred approximately 10,000 years ago as a response to climate change. At our site the chloride concentration increase in the upper aquifer was inferred to have occurred since 3000 years. The slightly different timing of chloride concentration increase in the upper aquifer is most likely because there is a time lag between the moment of recharge and the arrival of the more saline water at the bottom of the upper aquifer (Figures 1(a) and 1(b)). Palaeoclimate studies indicate drying of the climate over the last approximately 20,000 years, with current arid climatic conditions present since 4000 years [95–97].

While there is still some uncertainty regarding the porosity that is accessible to anions in clays and initial transport parameters of helium are difficult to constrain using independent evidence [10], the use of both chloride and helium at this location in central Australia provided independent information about the hydrological conditions and helped constrain the models that fit the solute profiles. Helium being produced *in situ* and influenced by groundwater residence time provided evidence of solute transport rates and processes, while chloride, besides providing evidence of solute transport, also provided insight into palaeohydrological conditions. This provides the natural background connectivity between the GAB and the Arckaringa Basin at the study site prior to further development of hydrocarbon resources mining or other changes.

6. Conclusions

This *in situ* study examined solute transport processes in an aquitard separating the GAB and the Arckaringa Basin using chloride and helium to determine if these tracers can be used in Australian case studies to examine vertical groundwater flow between these basins and, therefore, to help understand the effects of groundwater abstraction for mining water supply as well as investigate the potential use of these tracers in high level radioactive waste storage viability studies within central Australia.

The method worked at this location in central Australia with the use of chloride and helium. A match between a realistic model and both tracers is considered a valid representation of the site. The use of both chloride and helium concurrently limited the models that fit the data to the final model presented.

The final model that provided the best fit with both the chloride and helium profile was an initial steady state model that required a component of vertical groundwater flow through the aquitard. The vertical flow is very slow, only 0.7 mm/yr, but that controls the solute profile as well as diffusion. Therefore, solute transport is controlled by both diffusion and advection in this location. The upper section of the chloride profile requires an increase in chloride concentration since 3000 years ago in the upper aquifer. The chloride concentration increase at that time is almost certainly due to concentration of chloride in recharging groundwater due to the climate becoming more arid. The lower section of the profile is matched by an increase in both chloride and helium due to the onset of pumping in 2008 to provide groundwater to the Prominent Hill mine. Large volume groundwater extraction caused groundwater to be extracted from a stagnant zone and/or from the basement below with higher chloride and especially helium concentrations.

The hydraulic head profile shows that the drawdown response from pumping has already penetrated and moved through the aquitard. However, subsequent increase in chloride and helium concentration, from pumping in the lower aquifer, has not penetrated very far into the aquitard because the pressure response is much quicker than the solute transport through the aquitard (against downward flow).

From this study, we find the natural vertical groundwater flow velocity from the GAB to the Arckaringa Basin to be 0.7 mm/yr at the study site. Other studies of consolidated aquitards undertaken in cold or temperate climates also find solute transport controlled by diffusion with advective flow rates generally below 1 mm/yr [10, 27, 43, 98]. The aquitard properties and hydraulic head measurements gave

an instantaneous picture of vertical groundwater flow at the time of sampling and are an important element in the discussion. However, for a long-term perspective it is necessary to use environmental tracer profiles. Chloride and helium are useful tracers for understanding groundwater flow conditions in arid zones and temperate climates. Chloride is also useful for understanding palaeohydrological conditions in arid zones because its concentration varies considerably due to high evapotranspiration compared to precipitation concentrating solutes in recharging groundwater. Therefore, both approaches are needed to investigate vertical groundwater flow and solute transport. In addition, it has been advantageous to look at both chloride and helium concentration in our study area.

Conflicts of Interest

The authors declare that they have no conflicts of interest.

Acknowledgments

This study and paper were funded by the Government of South Australia's Department of Environment, Water and Natural Resources (DEWNR), Australia, under its Bioregional Assessment Program on the Arckaringa Basin. The authors would like to thank AINSE Ltd. for providing financial assistance (award: PGRA) to Stacey Priestley. Noble gases analysis was completed at the Noble Gas Lab at the Lamont-Doherty Earth Observatory, New York, and the authors thank Linda Baker for help with analysis. The authors thank the traditional owners and custodians (past and present) of the South Australian spring country, particularly the Antakirinja people. They also thank the pastoralist and graziers of the southwestern GAB, in particular Millers Creek Station. Finally, they thank OZ Minerals for allowing access to their mine water supply wells.

References

[1] W. Back, "Role of aquitards in hydrogeochemical systems: a synopsis," *Applied Geochemistry*, vol. 1, no. 3, pp. 427–437, 1986.

[2] J. A. Cherry and B. L. Parker, *Role of Aquitards in the Protection of Aquifers from Contamination: A "State of Science" Report*, vol. 47, AWWA Research Foundation, Denver, Colorado, Colo, USA, 2004.

[3] J. Park, C. M. Bethke, T. Torgersen, and T. M. Johnson, "Transport modeling applied to the interpretation of groundwater 36Cl age," *Water Resources Research*, vol. 38, no. 5, pp. 11–115, 2002.

[4] W. E. Sanford, "Correcting for diffusion in carbon-14 dating of ground water," *Groundwater*, vol. 35, no. 2, pp. 357–361, 1997.

[5] M. J. Hendry, D. K. Solomon, M. Person et al., "Can argillaceous formations isolate nuclear waste? Insights from isotopic, noble gas, and geochemical profiles," *Geofluids*, vol. 15, no. 3, pp. 381–386, 2015.

[6] F. Larroque, O. Cabaret, O. Atteia, A. Dupuy, and M. Franceschi, "Vertical heterogeneities of hydraulic aquitard parameters: preliminary results from laboratory and in situ monitoring," *Hydrological Sciences Journal*, vol. 58, no. 4, pp. 912–929, 2013.

[7] B. D. Smerdon, L. A. Smith, G. A. Harrington, W. P. Gardner, C. D. Piane, and J. Sarout, "Estimating the hydraulic properties of an aquitard from in situ pore pressure measurements," *Hydrogeology Journal*, vol. 22, no. 8, pp. 1875–1887, 2014.

[8] J. Batlle-Aguilar, P. G. Cook, and G. A. Harrington, "Comparison of hydraulic and chemical methods for determining hydraulic conductivity and leakage rates in argillaceous aquitards," *Journal of Hydrology*, vol. 532, pp. 102–121, 2016.

[9] C. E. Neuzil and J. D. Bredehoeft, "Measurement of in-situ hydraulic conductivity in the cretaceous Pierre Shale," in *Proceedings of the 3rd Invitational Well-Testing Symposium: Well Testing in Low Permeability Environments*, Berkeley, California, , Calif, USA, 1980.

[10] M. Mazurek, P. Alt-Epping, A. Bath et al., "Natural tracer profiles across argillaceous formations," *Applied Geochemistry*, vol. 26, no. 7, pp. 1035–1064, 2011.

[11] A. L. Herczeg, S. S. Dogramaci, and F. W. J. Leaney, "Origin of dissolved salts in a large, semi-arid groundwater system: murray Basin, Australia," *Marine & Freshwater Research*, vol. 52, no. 1, pp. 41–52, 2001.

[12] R. Kipfer, W. Aeschbach-Hertig, F. Peeters, and M. Stute, "Noble Gases in Lakes and Ground Waters," *Reviews in Mineralogy and Geochemistry*, vol. 47, no. 1, pp. 615–700, 2002.

[13] P. Trinchero, A. Delos, J. Molinero, M. Dentz, and P. Pitkänen, "Understanding and modelling dissolved gas transport in the bedrock of three Fennoscandian sites," *Journal of Hydrology*, vol. 512, pp. 506–517, 2014.

[14] D. I. Norman and J. A. Musgrave, "N2-Ar-He compositions in fluid inclusions: indicators of fluid source," *Geochimica et Cosmochimica Acta*, vol. 58, no. 3, pp. 1119–1131, 1994.

[15] K. Osenbrück, J. Lippmann, and C. Sonntag, "Dating very old pore waters in impermeable rocks by noble gas isotopes," *Geochimica et Cosmochimica Acta*, vol. 62, no. 18, pp. 3041–3045, 1998.

[16] S. Ali, M. Stute, T. Torgersen, G. Winckler, and B. M. Kennedy, "Helium measurements of pore fluids obtained from the San Andreas Fault Observatory at Depth (SAFOD, USA) drill cores," *Hydrogeology Journal*, vol. 19, no. 1, pp. 237–247, 2011.

[17] A. P. Rübel, C. Sonntag, J. Lippmann, F. J. Pearson, and A. Gautschi, "Solute transport in formations of very low permeability: Profiles of stable isotope and dissolved noble gas contents of pore water in the Opalinus Clay, Mont Terri, Switzerland," *Geochimica et Cosmochimica Acta*, vol. 66, no. 8, pp. 1311–1321, 2002.

[18] F. Bensenouci, J. L. Michelot, J. M. Matray et al., "A profile of helium-4 concentration in pore-water for assessing the transport phenomena through an argillaceous formation (Tournemire, France)," *Physics and Chemistry of the Earth*, vol. 36, no. 17-18, pp. 1521–1530, 2011.

[19] M. Mazurek, P. Alt-Epping, T. Gimmi et al., "Tracer profiles across argillaceous formations: a tool to constrain transport processes," in *Proceedings of the 12th International Symposium on Water-Rock Interaction, WRI-12*, pp. 767–771, chn, August 2007.

[20] A. L. Sheldon, D. K. Solomon, R. J. Poreda, and A. Hunt, "Radiogenic helium in shallow groundwater within a clay till, southwestern Ontario," *Water Resources Research*, vol. 39, no. 12, pp. HWC11–HWC112, 2003.

[21] I. D. Clark, T. Al, M. Jensen et al., "Paleozoic-aged brine and authigenic helium preserved in an Ordovician shale aquiclude," *Geology*, vol. 41, no. 9, pp. 951–954, 2013.

[22] T. Torgersen and W. B. Clarke, "Helium accumulation in groundwater, I: An evaluation of sources and the continental flux of crustal ^{4}He in the Great Artesian Basin, Australia," *Geochimica et Cosmochimica Acta*, vol. 49, no. 5, pp. 1211–1218, 1985.

[23] T. Torgersen and M. Stute, *Isotope Methods for Dating Old Groundwater*, International Atomic Energy Agency, Vienna, Austria, 2013.

[24] G. A. Harrington, W. P. Gardner, B. D. Smerdon, and M. J. Hendry, "Palaeohydrogeological insights from natural tracer profiles in aquitard porewater, Great Artesian Basin, Australia," *Water Resources Research*, vol. 49, no. 7, pp. 4054–4070, 2013.

[25] D. E. Desaulniers, J. A. Cherry, and P. Fritz, "Origin, age and movement of pore water in argillaceous Quaternary deposits at four sites in southwestern Ontario," *Journal of Hydrology*, vol. 50, no. C, pp. 231–257, 1981.

[26] D. E. Desaulniers and J. A. Cherry, "Origin and movement of groundwater and major ions in a thick deposit of Champlain Sea clay near Montreal," *Canadian Geotechnical Journal*, vol. 26, no. 1, pp. 80–89, 1989.

[27] V. H. Remenda, G. Van Der Kamp, and J. A. Cherry, "Use of vertical profiles of δ18O to constrain estimates of hydraulic conductivity in a thick, unfractured aquitard," *Water Resources Research*, vol. 32, no. 10, pp. 2979–2987, 1996.

[28] M. J. Hendry, S. L. Barbour, J. Zettl, V. Chostner, and L. I. Wassenaar, "Controls on the long-term downward transport of δ2H of water in a regionally extensive, two-layered aquitard system," *Water Resources Research*, vol. 47, no. 6, Article ID W06505, 2011.

[29] M. J. Hendry and L. I. Wassenaar, "Implications of the distribution of σD in pore waters for groundwater flow and the timing of geologic events in a thick aquitard system," *Water Resources Research*, vol. 35, no. 6, pp. 1751–1760, 1999.

[30] M. J. Hendry, S. L. Barbour, K. Novakowski, and L. I. Wassenaar, "Paleohydrogeology of the Cretaceous sediments of the Williston Basin using stable isotopes of water," *Water Resources Research*, vol. 49, no. 8, pp. 4580–4592, 2013.

[31] M. J. Hendry, C. J. Kelln, L. I. Wassenaar, and J. Shaw, "Characterizing the hydrogeology of a complex clay-rich aquitard system using detailed vertical profiles of the stable isotopes of water," *Journal of Hydrology*, vol. 293, no. 1-4, pp. 47–56, 2004.

[32] M. J. Hendry and L. I. Wassenaar, "Controls on the distribution of major ions in pore waters of a thick surficial aquitard," *Water Resources Research*, vol. 36, no. 2, pp. 503–513, 2000.

[33] T. A. Al, I. D. Clark, L. Kennell, M. Jensen, and K. G. Raven, "Geochemical evolution and residence time of porewater in low-permeability rocks of the Michigan Basin, Southwest Ontario," *Chemical Geology*, vol. 404, pp. 1–17, 2015.

[34] L. F. Konikow and J. R. Arévalo, "Advection and diffusion in a variable-salinity confining layer," *Water Resources Research*, vol. 29, no. 8, pp. 2747–2761, 1993.

[35] M. Mazurek, P. Alt-Epping, A. Bath, T. Gimmi, and H. N. Waber, *Natural Tracer Profiles Across Argillaceous Formations: The CLAYTRAC Project*, OECD Publishing, Paris, France, 2009.

[36] T. Gimmi, H. N. Waber, A. Gautschi, and A. Rübel, "Stable water isotopes in pore water of Jurassic argillaceous rocks as tracers for solute transport over large spatial and temporal scales," *Water Resources Research*, vol. 43, no. 4, Article ID W04410, 2007.

[37] M. Koroleva, P. Alt-Epping, and M. Mazurek, "Large-scale tracer profiles in a deep claystone formation (Opalinus Clay at Mont Russelin, Switzerland): Implications for solute transport processes and transport properties of the rock," *Chemical Geology*, vol. 280, no. 3-4, pp. 284–296, 2011.

[38] D. Patriarche, E. Ledoux, J.-L. Michelot, R. Simon-Coinçon, and S. Savoye, "Diffusion as the main process for mass transport in very low water content argillites: 2. Fluid flow and mass transport modeling," *Water Resources Research*, vol. 40, no. 1, pp. W015171–W0151715, 2004.

[39] D. Patriarche, J.-L. Michelot, E. Ledoux, and S. Savoye, "Diffusion as the main process for mass transport in very low water content argillites: 1. Chloride as a natural tracer for mass transport - Diffusion coefficient and concentration measurements in interstitial water," *Water Resources Research*, vol. 40, no. 1, pp. W015161–W0151619, 2004.

[40] W. E. Falck, A. H. Bath, and P. J. Hooker, "in Zeitschrift Der DeutschenGeologischenGesellschaft," *in Zeitschrift Der DeutschenGeologischenGesellschaft*, vol. 141, pp. 415–426, 1990.

[41] F. Bensenouci, J. L. Michelot, J. M. Matray, S. Savoye, J. Tremosa, and S. Gaboreau, "Profiles of chloride and stable isotopes in pore-water obtained from a 2000m-deep borehole through the Mesozoic sedimentary series in the eastern Paris Basin," *Physics and Chemistry of the Earth*, vol. 65, pp. 1–10, 2013.

[42] S. Savoye, J.-L. Michelot, F. Bensenouci, J.-M. Matray, and J. Cabrera, "Transfers through argillaceous rocks over large space and time scales: Insights given by water stable isotopes," *Physics and Chemistry of the Earth*, vol. 33, no. 1, pp. S67–S74, 2008.

[43] G. A. Harrington, A. J. Love, and A. L. Herczeg, "Relative importance of physical and geochemical processes affecting solute distributions in a clay aquitard," in *Water-Rock Interaction*, R. Cidu, Ed., pp. 177–180, A. A. Balkema Publishers, Leiden, Netherland, 2001.

[44] A. J. Love, A. L. Herczeg, and G. Walker, "Transport of water and solutes across a regional aquitard inferred from deuterium and chloride profiles Otway Basin, Australia," in *Proceedings of the in Isotopes in Water Resources Management Symposium*, 1996.

[45] A. L. Herczeg and F. W. Leaney, "Review: Environmental tracers in arid-zone hydrology," *Hydrogeology Journal*, vol. 19, no. 1, pp. 17–29, 2011.

[46] W. P. Gardner, G. A. Harrington, and B. D. Smerdon, "Using excess 4He to quantify variability in aquitard leakage," *Journal of Hydrology*, vol. 468-469, pp. 63–75, 2012.

[47] T. Hasegawa, K. Nakata, Y. Mahara, M. A. Habermehl, T. Oyama, and T. Higashihara, "Characterization of a diffusion-dominant system using chloride and chlorine isotopes (36Cl, 37Cl) for the confining layer of the Great Artesian Basin, Australia," *Geochimica et Cosmochimica Acta*, vol. 192, pp. 279–294, 2016.

[48] B. F. Jones, J. S. Hanor, and W. R. Evans, "Sources of dissolved salts in the central Murray Basin, Australia," *Chemical Geology*, vol. 111, no. 1-4, pp. 135–154, 1994.

[49] S. C. Priestley, D. L. Wohling, M. N. Keppel et al., "Detecting inter-aquifer leakage in areas with limited data using hydraulics and multiple environmental tracers, including ^{4}He, ^{36}Cl/Cl, ^{14}C and ^{87}Sr/^{86}Sr," *Hydrogeology Journal*, pp. 1–17, 2017.

[50] M. J. Hendry, E. Schmeling, L. I. Wassenaar, S. L. Barbour, and D. Pratt, "Determining the stable isotope composition of pore water from saturated and unsaturated zone core: Improvements to the direct vapour equilibration laser spectrometry method," *Hydrology and Earth System Sciences*, vol. 19, no. 11, pp. 4427–4440, 2015.

[51] C. Zheng and P. P. Wang, *MT3DMS: A Modular Three-Dimensional Multispecies Transport Model for Simulation of*

Advection, Dispersion, and Chemical Reactions of Contaminants in Groundwater Systems; Documentation and User's Guide, Strategic Environmental Research and Development Program, U.S. Army Corps of Engineers, Washington, Wash, USA, 1999.

[52] D. K. Solomon, A. Hunt, and R. J. Poreda, "Source of radiogenic helium 4 in shallow aquifers: implications for dating young groundwater," *Water Resources Research*, vol. 32, no. 6, pp. 1805–1813, 1996.

[53] T. Kleinig, S. C. Priestley, D. Wohling, and N. I. Robinson, *Arckaringa Basin aquifer connectivity*, Government of South Australia, through Department of Environment, Water and Natural Resources, Adelaide, Australia, 2015.

[54] D. Wohling, M. Keppel, S. Fulton, A. Costar, L. Sampson, and V. Berens, *Australian Initiative on Coal Seam Gas and Large Coal Mining - Arckaringa Basin and Pedirka Basin Groundwater Assessment Projects*, Government of South Australia, through Department of Environment, Water and Natural Resources, Adelaide, 2013.

[55] G. J. Ambrose and R. B. Flint, Billa Kalina, South Australia, Explanatory Notes. 1:250 000 geological series, geological sheet SH 53-7, Geological Survey of South Australia, 1980.

[56] K. Gallagher and K. Lambeck, "Subsidence, sedimentation and sea-level changes in the Eromanga Basin, Australia," *Basin Research*, vol. 2, no. 2, pp. 115–131, 1989.

[57] B. R. Senior, A. Mond, and P. L. Harrison, *Geology of the Eromanga Basin*, Bureau of Mineral Resources, Geology and Geophysics, Canberra, Australia, 1978.

[58] D. Toupin, P. J. Eadington, M. Person, P. Morin, J. Wieck, and D. Warner, "Petroleum hydrogeology of the Cooper and Eromanga basins, Australia: some insights from mathematical modeling and fluid inclusion data," *AAPG Bulletin*, vol. 81, no. 4, pp. 577–603, 1997.

[59] A. J. A. J. Love, D. Wohling, S. Fulton, P. Rousseau-Gueutin, and S. D. Ritter, *Allocating Water and Maintaining Springs in the Great Artesian Basin, Volume II: Groundwater Recharge, Hydrodynamics and Hydrochemistry of the Western Great Artesian Basin*, National Water Commission, Canberra, Australia, 2013.

[60] H. Wopfner and C. R. Twidale, *New Zealand Geographer*, J. N. Jennings and J. A. Mabbutt, Eds., vol. 23 of *chapter 7*, Landform studies from Australia and New Guinea, 1967.

[61] R. J. Allan, *Natural History of the North East Deserts*, M. J. Tyler, C. R. Twidale, M. Davies, and C. B. Wells, Eds., chapter 9, Royal Society of South Australia Inc., Adelaide, Australia, 1990.

[62] P. B. McMahon, "Aquifer/aquitard interfaces: Mixing zones that enhance biogeochemical reactions," *Hydrogeology Journal*, vol. 9, no. 1, pp. 34–43, 2001.

[63] M. Keppel, B. Jensen-Schmidt, D. Wohling, and L. Sampson, *A hydrogeological characterisation of the Arckaringa Basin*, Government of South Australia, through Department of Environment, Water and Natural Resources, Adelaide, Australia, 2015.

[64] SKM, Prominent Hill Mine Groundwater Model Update (PH5), Prepared for OZ Minerals, Project Number VE23146.600, 2010.

[65] L. I. Wassenaar, M. J. Hendry, V. L. Chostner, and G. P. Lis, "High resolution pore water δ^2H and δ^{18}O measurements by H_2O(liquid)-H_2O (vapor) equilibration laser spectroscopy," *Environmental Science & Technology*, vol. 42, no. 24, pp. 9262–9267, 2008.

[66] U. Beyerle, W. Aeschbach-Hertig, D. M. Imboden, H. Baur, T. Graf, and R. Kipfer, "A mass, spectrometric system for the analysis of noble gases and tritium from water samples," *Environmental Science & Technology*, vol. 34, no. 10, pp. 2042–2050, 2000.

[67] R. F. Weiss, "Piggyback sampler for dissolved gas studies on sealed water samples," *Deep-Sea Research and Oceanographic Abstracts*, vol. 15, no. 6, pp. 695–699, 1968.

[68] APHA, *Standard Methods for the Examination of Water and Waste Water*, vol. 56, American Public Health Association, Washington, Wash, USA, 20th edition, 1998.

[69] E. Sacchi, J.-L. Michelot, H. Pitsch, P. Lalieux, and J.-F. Aranyossy, "Extraction of water and solutes from argillaceous rocks for geochemical characterisation: methods, processes, and current understanding," *Hydrogeology Journal*, vol. 9, no. 1, pp. 17–33, 2001.

[70] S. T. Horseman, J. J. W. Higgo, J. Alexander, and J. F. Harrington, "Water, gas and solute movement through argillaceous media, Nuclear Energy Agency REP," *Water, gas and solute movement through argillaceous media, Nuclear Energy Agency REP*, 1996.

[71] F. J. Pearson, "What is the porosity of a mudrock?" *Geological Society, London, Special Publications*, vol. 158, pp. 9–21, 1999.

[72] H. N. Waber and J. A. T. Smellie, "Characterisation of pore water in crystalline rocks," *Applied Geochemistry*, vol. 23, no. 7, pp. 1834–1861, 2008.

[73] L. R. Van Loon, M. A. Glaus, and W. Müller, "Anion exclusion effects in compacted bentonites: towards a better understanding of anion diffusion," *Applied Geochemistry*, vol. 22, no. 11, pp. 2536–2552, 2007.

[74] M. J. Hendry and G. A. Harrington, "Comparing vertical profiles of natural tracers in the Williston Basin to estimate the onset of deep aquifer activation," *Water Resources Research*, vol. 50, no. 8, pp. 6496–6506, 2014.

[75] Standards Australia, Method of testing soils for engineering purposes, AS 1289.0—2000, Council of Standards Australia, New South Wales, 2000.

[76] Standards Australia, Method of testing soils for engineering purposes, AS 1289.0—1999, Council of Standards Australia, New South Wales, 1999.

[77] M. Stute, M. Forster, H. Frischkorn et al., "Cooling of tropical Brazil (5°C) during the last glacial maximum," *Science*, vol. 269, no. 5222, pp. 379–383, 1995.

[78] C. J. Ballentine, R. Burgess, and B. Marty, *Noble Gases in Geochemistry and Cosmochemistry*, D. Porcelli, C. J. Ballentine, and R. Wieler, Eds., vol. 47, 2002.

[79] P. Grathwohl, *Diffusion in natural porous media: contaminant transport, sorption/desorption and dissolution kinetics*, Springer Science+Business Media, LLC, New York, NY, USA, 1958.

[80] , *Environmental Tracers in Subsurface Hydrology*, P. G. Cook and A. L. Herczeg, Eds., Springer Science+Business Media, New York, NY, USA, 2000.

[81] B. Jähne, G. Heinz, and W. Dietrich, "Measurement of the diffusion coefficients of sparingly soluble gases in water," *Journal of Geophysical Research: Oceans*, vol. 92, no. 10, pp. 10767–10776, 1987.

[82] L. Yuan-Hui and S. Gregory, "Diffusion of ions in sea water and in deep-sea sediments," *Geochimica et Cosmochimica Acta*, vol. 38, no. 5, pp. 703–714, 1974.

[83] T. Torgersen, "Controls on pore-fluid concentration of 4He and 222Rn and the calculation of 4He/222Rn ages," *Journal of Geochemical Exploration*, vol. 13, no. 1, pp. 57–75, 1980.

[84] M. Huysmans and A. Dassargues, "Review of the use of Péclet numbers to determine the relative importance of advection and diffusion in low permeability environments," *Hydrogeology Journal*, vol. 13, no. 5-6, pp. 895–904, 2005.

[85] X. Zhao, T. L. B. Fritzel, H. A. M. Quinodoz, C. M. Bethke, and T. Torgersen, "Controls on the distribution and isotopic composition of helium in deep ground-water flows," *Geology*, vol. 26, no. 4, pp. 291–294, 1998.

[86] B. Barnett, L. R. Townley, V. Post et al., *Australian groundwater modelling guidelines*, Waterlines report National Water Commission, Canberra, Australia, 2012.

[87] C. M. Bethke, X. Zhao, and T. Torgersen, "Groundwater flow and the 4He distribution in the Great Artesian Basin of Australia," *Journal of Geophysical Research: Solid Earth*, vol. 104, no. 6, Article ID 1999JB900085, pp. 12999–13011, 1999.

[88] U. Beyerle, W. Aeschbach-Hertig, R. Kipfer et al., "Noble gas data from the Great Artesian Basin provide a temperature record of Australia on time scales of 10^5 years," in *Proceedings of the International Symposium on Isotope Techniques in Water Resources Development and Management*, vol. 43, pp. 19–24, 1999.

[89] B. E. Lehmann, A. Love, R. Purtschert et al., "A comparison of groundwater dating with 81Kr, 36Cl and 4He in four wells of the Great Artesian Basin, Australia," *Earth and Planetary Science Letters*, vol. 211, no. 3-4, pp. 237–250, 2003.

[90] Y. Mahara, M. A. Habermehl, T. Hasegawa et al., "Groundwater dating by estimation of groundwater flow velocity and dissolved 4He accumulation rate calibrated by 36Cl in the Great Artesian Basin, Australia," *Earth and Planetary Science Letters*, vol. 287, no. 1-2, pp. 43–56, 2009.

[91] G. R. Walker and P. G. Cook, "The importance of considering diffusion when using carbon-14 to estimate groundwater recharge to an unconfined aquifer," *Journal of Hydrology*, vol. 128, no. 1-4, pp. 41–48, 1991.

[92] M. J. Currell, P. Dahlhaus, and H. Ii, "Stable isotopes as indicators of water and salinity sources in a southeast Australian coastal wetland: identifying relict marine water, and implications for future change," *Hydrogeology Journal*, vol. 23, no. 2, pp. 235–248, 2015.

[93] G. B. Allison and M. W. Hughes, "The use of natural tracers as indicators of soil-water movement in a temperate semi-arid region," *Journal of Hydrology*, vol. 60, no. 1-4, pp. 157–173, 1983.

[94] B. Petrides, I. Cartwright, and T. R. Weaver, "The evolution of groundwater in the Tyrrell catchment, south-central Murray Basin, Victoria, Australia," *Hydrogeology Journal*, vol. 14, no. 8, pp. 1522–1543, 2006.

[95] T. J. Cohen, G. C. Nanson, J. D. Jansen et al., "Continental aridification and the vanishing of Australia's megalakes," *Geology*, vol. 39, no. 2, pp. 167–170, 2011.

[96] P. P. Hesse, J. W. Magee, and S. van der Kaars, "Late Quaternary climates of the Australian arid zone: A review," *Quaternary International*, vol. 118-119, pp. 87–102, 2004.

[97] J. W. Magee, G. H. Miller, N. A. Spooner, and D. Questiaux, "Continuous 150 k.y. monsoon record from Lake Eyre, Australia: insolation-forcing implications and unexpected Holocene failure," *Geology*, vol. 32, no. 10, pp. 885–888, 2004.

[98] R. Joel Shaw and M. Jim Hendry, "Hydrogeology of a thick clay till and Cretaceous clay sequence, Saskatchewan, Canada," *Canadian Geotechnical Journal*, vol. 35, no. 6, pp. 1041–1052, 1998.